

See discussions, stats, and author profiles for this publication at: <https://www.researchgate.net/publication/234985349>

Ferroelectric to Relaxor Crossover and Dielectric Phase Diagram in the BaTiO₃–BaSnO₃ System

ARTICLE *in* JOURNAL OF APPLIED PHYSICS · APRIL 2007

Impact Factor: 2.18 · DOI: 10.1063/1.2715522

CITATIONS

68

READS

273

3 AUTHORS, INCLUDING:



Alexei A Bokov

Simon Fraser University

116 PUBLICATIONS 2,780 CITATIONS

SEE PROFILE

Ferroelectric to relaxor crossover and dielectric phase diagram in the $\text{BaTiO}_3\text{--BaSnO}_3$ system

C. Lei, A. A. Bokov, and Z.-G. Ye^{a)}*Department of Chemistry, Simon Fraser University, 8888 University Drive, Burnaby, British Columbia V5A 1S6, Canada*

(Received 10 November 2006; accepted 26 January 2007; published online 19 April 2007)

The $(1-x)\text{BaTiO}_3\text{--}x\text{BaSnO}_3$ ($0 \leq x \leq 0.30$) perovskite solid solution ceramics were prepared by solid state reaction and studied by dielectric spectroscopy. The complex dielectric permittivity was measured as a function of frequency (0.1 Hz–100 kHz) in the temperature (T) range of 123–573 K. The transition from the high-temperature paraelectric state where the dielectric constant obeys the Curie-Weiss law to the ergodic cluster state is found to occur at the same temperature of 485 K in all the compositions of $x \geq 0.04$ and at lower temperatures in those with a smaller x . For $0 \leq x \leq x_c = 0.19$, the temperature of the dielectric peak T_m , corresponding to the diffuse transition from the ergodic polar cluster state to the ferroelectric state, decreases with increasing x and does not depend on frequency. The diffuseness of the peak gradually increases. For $x > x_c$, the permittivity exhibits relaxor behavior with the frequency-dependent T_m satisfying the Vogel-Fulcher law. The temperature variation of the permittivity on the high-temperature slope of the peak ($T > T_m$) is characterized by the characteristic Lorenz-type quadratic law for relaxors, with the diffuseness increasing with the increase of x . The mechanisms of the dielectric response in different parts of the phase diagram are discussed. In particular, the crossover from diffuse ferroelectric phase transition to relaxor ferroelectric behavior is attributed to the appearance at $x > x_c$ of the additional dielectric contribution arising from the flipping of the local polarization of the polar clusters. The temperature-composition phase diagram of the $\text{Ba}(\text{Ti}_{1-x}\text{Sn}_x)\text{O}_3$ system has been established, which delimits the paraelectric, ergodic polar cluster, nonergodic ferroelectric, and relaxor phases (states) and indicates the crossover from ferroelectric to relaxor behavior at $x = x_c$. © 2007 American Institute of Physics. [DOI: 10.1063/1.2715522]

I. INTRODUCTION

Relaxor ferroelectrics (relaxors), characterized by a broad maximum in their dielectric permittivity versus temperature response and by the frequency dependence of the temperature of the permittivity peak (T_m), have attracted much attention both for fundamental research and for technological applications.^{1,2} In relaxors, a strong frequency dispersion is usually observed on the low-temperature slope of the dielectric peak, and T_m shifts to higher temperatures with increasing frequency, following the characteristic Vogel-Fulcher (VF) law.^{3,4} The very high dielectric permittivity in relaxors around the maximum makes them excellent materials for multilayered ceramic capacitors. Relaxors, such as $\text{Pb}(\text{Mg}_{1/3}\text{Nb}_{2/3})\text{O}_3$ (PMN), also exhibit very high electrostrictive effect.⁵

In some relaxors, no breakdown in the macroscopic crystal symmetry can be observed down to low temperatures. Thus, no ferroelectric (FE) phase transition occurs around T_m or below. However, a ferroelectric phase can be induced by the application of an external electric field.⁶ It should be noted that ferroelectrics with “diffuse phase transition” (DPT) are different from relaxors. They show no significant shift of T_m caused by frequency dispersion.⁷ Several models have been proposed to explain the relaxational behavior in relaxors.^{7–13} A common point of these models is the local

distortion of the structure due to chemical inhomogeneity, giving rise to polar clusters of nanometer size. These clusters were confirmed to exist in the classical relaxor, PMN, by means of the measurement of optic index of refraction,⁸ synchrotron x-ray scattering,¹⁴ diffuse neutron scattering, and transmission electron microscopy.^{15,16}

Many lead-based complex perovskites, such as PMN, $\text{Pb}(\text{Zn}_{1/3}\text{Nb}_{2/3})\text{O}_3$, and $(\text{Pb},\text{La})(\text{Zr},\text{Ti})\text{O}_3$ (PLZT),^{2,3,9} are known to exhibit relaxor behavior. However, lead is an environmental unfriendly element. Thus, lead-free materials are highly desirable, and barium titanate [BaTiO_3 (BT)], a well-known normal ferroelectric material, has attracted greater interest than ever. This revival of interest is mainly due to its lead-free character. Chemical substitutions on the B site have been carried out on BT with various cations, such as Zr,¹⁷ Hf,¹⁸ Ce,¹⁹ Y,²⁰ and Sn.²¹ The partial substitution of Sn^{4+} for Ti^{4+} in BT was reported by Smolenskii and Isupov²¹ to result in a ferroelectrics with DPT.²² The relaxor behavior of Sn-substitution BT (BTSn) system with high enough concentration of Sn was studied recently.²³ Similar relaxor properties are observed in some other BT-based solid solutions.^{17,19,20} It is clear that the relaxor behavior originates from compositional disorder, i.e., the disorder in the distribution of different ions over the similar crystallographic sites (e.g., Ti^{4+} and Sn^{4+} ions in BTSn or Mg^{2+} and Nb^{5+} ions in PMN). In the classical relaxors of lead-containing complex perovskite structure, the concentration of the disordered ions is pre-

^{a)}Electronic mail: zye@sfu.ca

scribed by the chemical stoichiometry and thus cannot be changed. Therefore the possibilities of investigating the relation between compositional disorder and relaxor phenomenon are limited. In the solid solutions with isovalent substitution (such as BTSn), different concentrations of ions and thereby various degrees of compositional disorder can be achieved. Consequently these solid solutions become very interesting for the study of the nature of relaxor ferroelectricity. Detailed and systematical investigations of substitutional effects and the crossover from the normal ferroelectric behavior in one of the end members of the solid solution to the relaxor behavior in compositions with large enough concentration of substituting ions are highly desirable. In the present work, the solid solution between BaTiO_3 and the nonferroelectric BaSnO_3 has been studied to illustrate these effects.

II. EXPERIMENTAL PROCEDURE

The ceramics of $(1-x)\text{BaTiO}_3-x\text{BaSnO}_3$ ($x=0-0.30$, abbreviated as BT for $x=0$ and BTSn100x for $x>0$) solid solution were prepared by solid state reactions. The starting materials, BaCO_3 (99.9%), TiO_2 (99.9%), and SnO_2 (99.9%), were mixed according to the stoichiometric compositions. After grinding, the mixed powder was pressed into disk-shaped pellets and calcined at 1100°C for 4 h. The calcined pellets were pulverized, ground with addition of a small amount of polyvinyl alcohol, and pressed into pellets of 10 mm in diameter. The pellets were then sintered at 1400°C for 4 h. Dense ceramics of good quality (with 92%–97% of the theoretical density) were obtained. The mean grain size of all the ceramic samples prepared was found to be between 50 and $100\text{ }\mu\text{m}$ by scanning electron microscopy (Bausch & Lomb Nanolab SEM), which is consistent with the previously published data on a similar BT-based system.²⁴ It is interesting to note that the density and grain size do not change with Sn content. X-ray diffraction (XRD) experiments were performed on a Rigaku diffractometer using $\text{Cu K}\alpha$ radiation. Both circular surfaces of the samples were polished with diamond past (down to $3\text{ }\mu\text{m}$), and then sputtered with gold layers to form electrodes for dielectric measurements. The complex dielectric permittivity was measured as a function of frequency (0.1 Hz–100 kHz) using a computer-controlled alpha dielectric analyzer (Novocontrol). The measurements were carried out in the temperature range between 573 and 123 K upon cooling with an accuracy better than 0.03 K. The measuring field strength was about 2 V/mm.

III. RESULTS AND ANALYSIS

The XRD results confirmed that all the $(1-x)\text{BaTiO}_3-x\text{BaSnO}_3$ ($x=0-0.30$) ceramics are of pure perovskite structure. The temperature dependences of the real part of dielectric permittivity (ϵ') measured at 100 kHz for the ceramics with selected concentrations x are shown in Fig. 1. Based on the dielectric measurement results, the phase diagram of the system has been established, as shown in Fig. 2. In the compositions of small x , the same dielectric anomalies as in pure BT are observed,²⁵ corresponding to the cubic

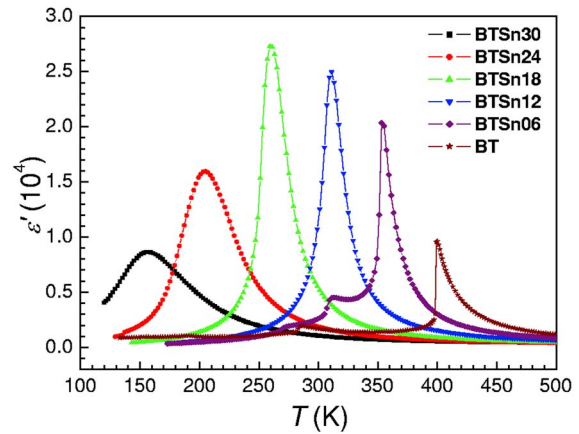


FIG. 1. (Color online) Temperature dependence of the dielectric constant (ϵ') measured at 100 kHz for the $(1-x)\text{BaTiO}_3-x\text{BaSnO}_3$ solid solution ceramics with $x=0, 0.06, 0.12, 0.18, 0.24$, and 0.30 .

to tetragonal (T_m), tetragonal to orthorhombic (T_2), and orthorhombic to rhombohedral (T_1) phase transitions. As the Sn content increases, T_m decreases while T_1 and T_2 increase and merge into T_m . This phase diagram basically agrees with the data reported in Ref. 21 and with the recently published data in terms of structural phase transition temperatures.^{23,26} T_m decreases linearly with increasing x , except for an inflection at about $x=0.19$. The decreasing rate, dT_m/dx , was found to be 7.6 K/mol % when $x<0.19$, but 9.5 K/mol % when $x>0.19$. The different states indicated in the phase diagram of Fig. 2 will be discussed in detail in the following text.

The temperature dependences of ϵ' and imaginary part of permittivity (ϵ'') for BT, BTSn06, BTSn20, and BTSn30

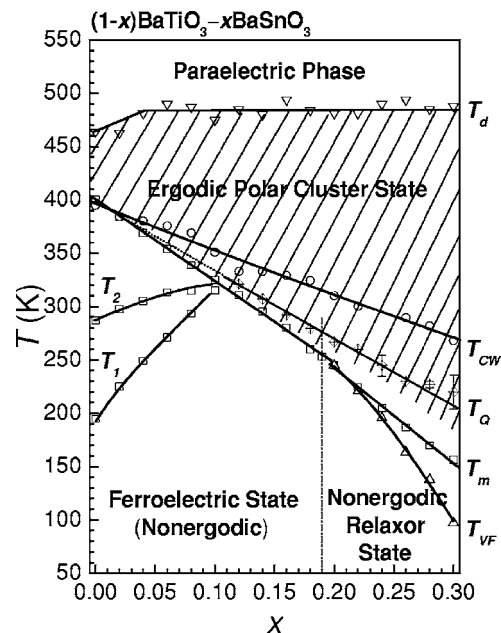


FIG. 2. Phase diagram of $(1-x)\text{BaTiO}_3-x\text{BaSnO}_3$ system established from dielectric spectroscopic analysis. T_m , T_1 , and T_2 are the temperatures of $\epsilon'(T)$ anomalies at 100 kHz. T_{VF} and T_{CW} are the characteristic temperatures obtained from Eqs. (1) and (3), respectively. T_d is the temperature below which deviation from the Curie-Weiss law, Eq. (3), occurs. T_Q is the temperature above which deviation from Eq. (2) occurs. The crossover concentration of $x_c=0.19$ is indicated by the dash-dot line.

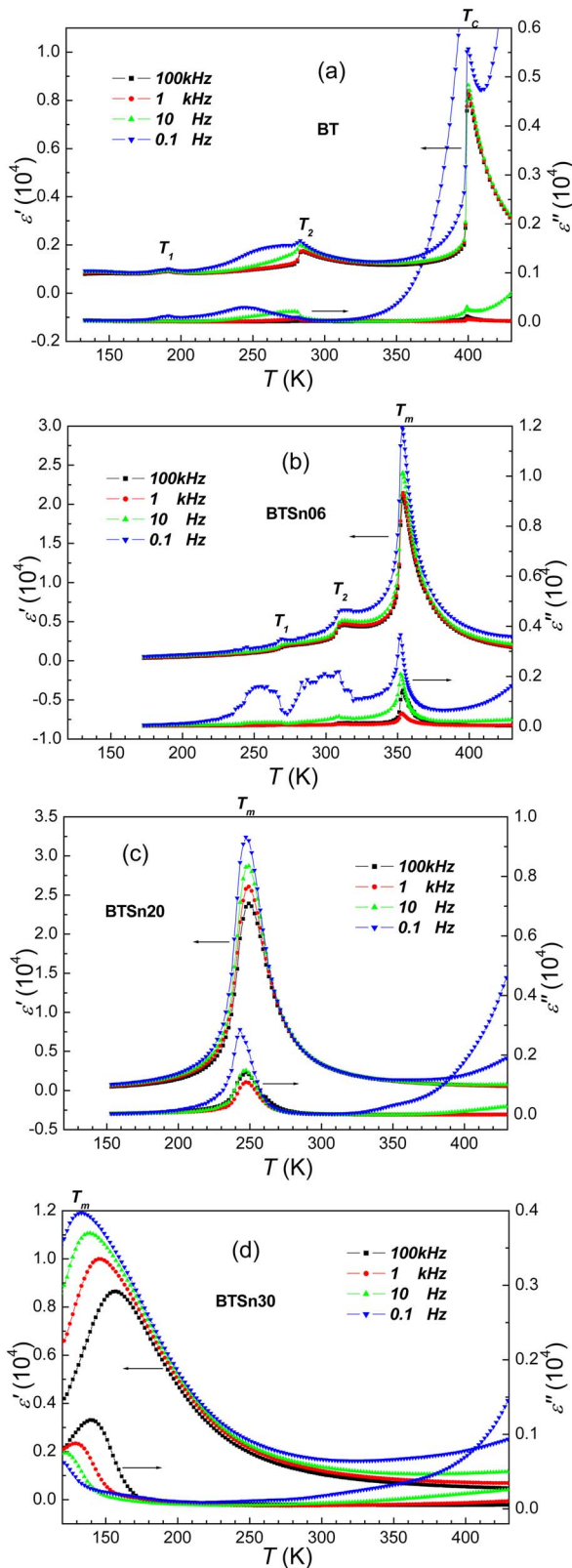


FIG. 3. (Color online) Temperature dependences of the real and imaginary parts of the dielectric permittivity of (a) BT, (b) BTSn06, (c) BTSn20, and (d) BTSn30 ceramics measured at different frequencies upon cooling.

at selected frequencies are shown in Fig. 3. At high temperatures, both the real and imaginary parts of the permittivity increase significantly, especially at low frequencies, indicating a strong dispersion. This dielectric contribution appears

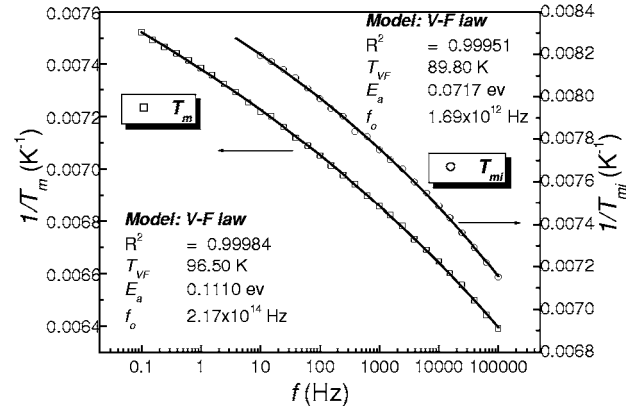


FIG. 4. The inverse temperatures of both the real and imaginary permittivity maxima, T_m and T_{mi} , as a function of frequency for the BTSn30 ceramics. Solid curves represent the fitting to the Vogel-Fulcher law. T_{mi} in the frequency range of 0.1–10 Hz is beyond the temperature range measured.

at ~ 300 K at 0.1 Hz in all the samples. Such kind of contribution is often observed at high temperatures in perovskite ceramics. It is most probably caused by the relaxation of mobile charge carriers and has no immediate relation to the ferroelectric phenomena. Therefore, we are not considering this dispersion in the present work.

As expected in the case of classical first-order displacive ferroelectric phase transition, pure BT shows a sharp $\varepsilon'(T)$ peak at the Curie point $T_C = T_m$ without significant dielectric dispersion (at T_m , $\tan \delta$ is about 0.8% at 1 kHz). Very large dispersion is observed around and below T_m in the samples with large x [see Fig. 3(d) as an example], strongly resembling the behavior in relaxor ferroelectrics. This crossover to relaxorlike behavior induced by increasing x is investigated here in detail.

The empirical VF law is used to characterize the frequency dispersion of T_m in relaxors:^{3,4}

$$f = f_0 \exp[-E_a/k(T_m - T_{VF})], \quad (1)$$

where f is the measurement frequency, and E_a , T_{VF} , and f_0 are the parameters. Figure 4 shows the frequency dependence of the reciprocal of T_m for the BTSn30 sample. The temperatures of both real and imaginary permittivity maxima, T_m and T_{mi} , fit well to the VF law. Similar fit was obtained for other compositions with large x . The parameters T_{VF} from the T_{mi} fitting were found to be about 10 K lower than that from the corresponding T_m fitting (which is characteristic of relaxors). The difference, $\Delta T_m = T_m(100 \text{ kHz}) - T_m(0.1 \text{ Hz})$, is 23.6 K in BTSn30, while it is only 1.9 K in BTSn20. For the compositions with $x \leq x_c = 0.19$, ΔT_m is close to zero (< 0.5 K), thus the VF fitting becomes irrelevant. Figures 2 and 5 show the parameters T_{VF} , E_a , and f_0 as a function of Sn content. The difference between T_{VF} and $T_m(100 \text{ kHz})$ gradually increases from 4.5 K for BTSn20 to 59.3 K for BTSn30, which reflects the same trend as the parameter ΔT_m . Similar relation between T_{VF} and T_m temperatures with changing x was observed also in the other BT-based solid solution systems, $\text{Ba}(\text{Ti}_{1-x}\text{Zr}_x)\text{O}_3$ and $\text{Ba}_{1-x/2}(\text{Ti}_{1-x}\text{Nb}_x)\text{O}_3$, and the merging point of the $T_{VF}(x)$ and $T_m(x)$ curves was considered as the ferroelectric-relaxor crossover composition.²⁷ However, it was found in those

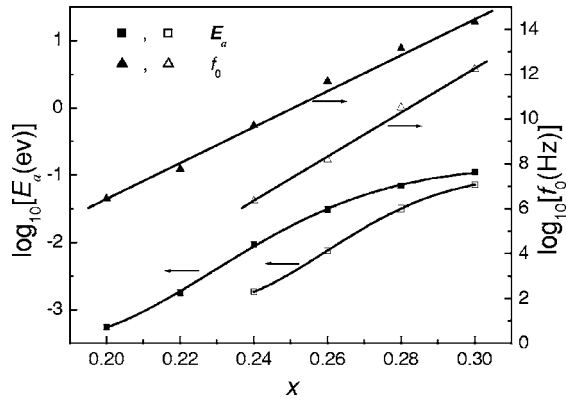


FIG. 5. Fitting parameters, E_a and f_0 [from Eq. (1)], as a function of the Sn content in the BT–BSn system. Filled and open symbols represent the fitting parameters for T_m and T_{mi} , respectively.

cases that the Vogel-Fulcher line $T_{VF}(x)$ (at $x > x_c$) was the best extrapolation of the ferroelectric line $T_m(x)$ (at $x < x_c$). This is evidently not the same case in the $\text{Ba}(\text{Ti}_{1-x}\text{Sn}_x)\text{O}_3$ system (see Fig. 2).

We recently proposed a quadratic formula to describe the dependence of the permittivity on temperature at $T > T_m$ in relaxors:^{28,29}

$$\frac{\varepsilon_A}{\varepsilon} = 1 + \frac{(T - T_A)^2}{2\delta^2}, \quad (2)$$

where ε_A , T_A , and δ are the parameters. The results of fitting to this law for the BTSn30 sample are shown in Fig. 6 as an example. An excellent fit is achieved in the temperature range from 164 K (slightly higher than $T_m = 156$ K) to 240 K. The deviation from the quadratic law near T_m is due to the conventional relaxor dispersion,^{28,29} which becomes significant below 164 K, while the discrepancy at high temperatures results from the gradual change to the Curie-Weiss (CW) law (see below). T_A was typically 2–8 K lower than T_m . The variation of T_Q [the temperature above which the deviation from Eq. (2) occurs] as a function of Sn content is plotted in Fig. 2. T_Q is slightly different in different samples

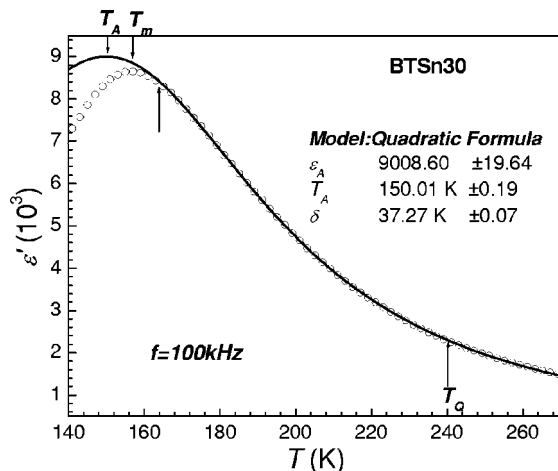


FIG. 6. Dielectric permittivity at 100 kHz vs temperature for the BTSn30 ceramics. Solid line represents the fitting to the quadratic law, Eq. (2). Upward arrows indicate the lower and upper temperatures from which the dielectric permittivity starts to deviate from Eq. (2).

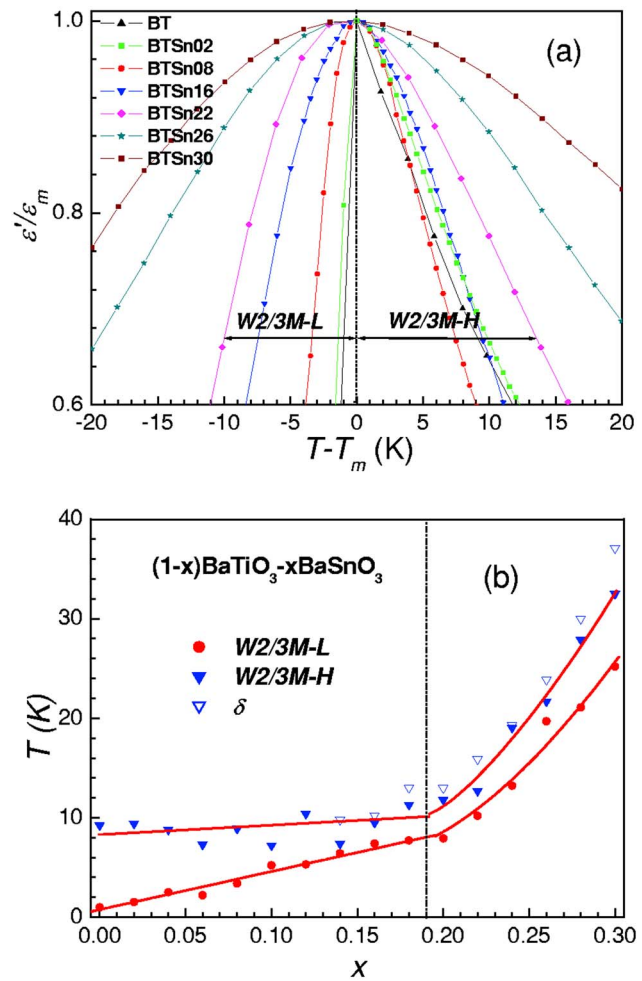


FIG. 7. (Color online) (a) Normalized real part of dielectric permittivity ($\varepsilon'/\varepsilon_m$) at 100 kHz as a function of $(T - T_m)$ and (b) parameters $W2/3M-L$, $W2/3M-H$, and δ as a function of the Sn content in the $(1-x)\text{BT}-x\text{BSn}$ system.

of the same composition, probably due to slight variation in the sample quality. Therefore, the average T_Q values were used to describe the variation of T_Q in Fig. 2. It shows that T_Q increases linearly with decreasing x and can be extrapolated to merge into T_C in pure BT. The frequency-independent parameter δ can be used to characterize the width (diffuseness) of the permittivity peak. The variation of δ as a function of x is displayed in Fig. 7(b). For the compositions with $x < 0.14$, fitting to Eq. (2) is insensible because the temperature range in which it is supposed to be valid becomes too narrow ($< \delta$). Therefore, to characterize the diffuseness some other way is needed. The width of the peak at 2/3 maximum is the alternative for this purpose. Since the peaks are evidently asymmetric, we introduce two parameters, $W2/3M-L$ and $W2/3M-H$, defined as the difference between T_m and the temperature where ε' reaches 2/3 of the maximum value from the low-temperature and the high-temperature sides of the peak, respectively, as shown in Fig. 7(a). The variations of these two parameters as a function of x are plotted in Fig. 7(b). One may notice that $W2/M-H$ is close to but slightly lower than δ , and this can be explained by the fact that the fitting parameters, ε_A and T_A , are close to $\varepsilon_m \equiv \varepsilon'(T_m)$ and T_m , respectively, as shown

in Fig. 6. For $x \leq x_c$, $W2/3M-L$ increases proportionally with increasing x , while $W2/3M-H$ remains almost unchanged, and both parameters increase steeply in the relaxor region with $x > x_c$. To analyze this behavior more closely, the normalized permittivity ($\varepsilon'/\varepsilon_m$) of selected compositions is plotted as a function of $(T-T_m)$ in Fig. 7(a). One can see that the sharpness of the peak gradually decreases with increasing x not only on the low-temperature side but also on the high-temperature side. At some compositions with nonzero x , $W2/3M-H$ can be even smaller than at $x=0$. This is because the Curie-Weiss-like shape in pure BT changes to quadratic-like shape in the compositions with large enough x . Given that $W2/3M-H$ is nonzero even for the pure BT, it is thus more meaningful to use $W2/3M-L$ as the parameter characterizing the diffuseness of ferroelectric DPT. Similar to the parameter δ , it describes the width of the temperature peak of the static dielectric permittivity. At $x > x_c$ the dispersion appears and the measured permittivity is no longer static. This is the possible reason (or one of the reasons) why $W2/3M-L$ increases more sharply at $x > x_c$.

The other empirical formula, namely, $\varepsilon_m/\varepsilon' - 1 \propto (T - T_m)^\gamma$ ($1 < \gamma < 2$), was sometimes used to describe the temperature variation of ε' at DPT. In particular, this formula has been applied to the BTSn solid solution.³⁰ Analysis of our experimental data for all concentrations $x > 0$ does not confirm the satisfaction of this relation in any reasonably wide temperature interval.

It is well accepted that for normal ferroelectrics the CW law is satisfied at $T > T_m$.^{25,31}

$$\varepsilon' = \varepsilon_0 + C/(T - T_{CW}), \quad (3)$$

where T_{CW} is the Curie-Weiss temperature, C the Curie constant, and ε_0 the parameter representing the possible temperature-independent (nonferroelectric) contribution to the permittivity (including the contribution of high-energy phonon modes and electronic polarization). The CW law is also observed in relaxor ferroelectrics,¹ but at temperatures much higher than T_m . In BTSn, the additional nonferroelectric polarization mechanism contributes to the dielectric permittivity at high temperatures and low frequencies (see above). Since this contribution is strongly temperature dependent, it cannot be described by the parameter ε_0 and thus can lead to a large error in the determination of the CW parameters. High enough frequencies at which this parasitic contribution becomes negligible are required to examine the CW law. Our data reveal that at a temperature as high as 570 K (the highest temperature used), the value of ε' decreases with increasing frequency and then the dependence flattens when $f > 1$ kHz, indicating that the data at $f > 1$ kHz are suitable for investigation. The reciprocal of $(\varepsilon' - \varepsilon_0)$ as a function of temperature at 100 kHz and the fitting to Eq. (3) for selected compositions are shown in Fig. 8(a). T_d is defined as the temperature below which the deviation from the CW law occurs. In order to illustrate the quality of fitting and to obtain the exact values of T_d , the fitting residuals, $(\varepsilon'_{\text{cal}} - \varepsilon)/\varepsilon'$ (where $\varepsilon'_{\text{cal}}$ is the trend given by the CW law), are shown in Fig. 8(b). It can be seen that the CW

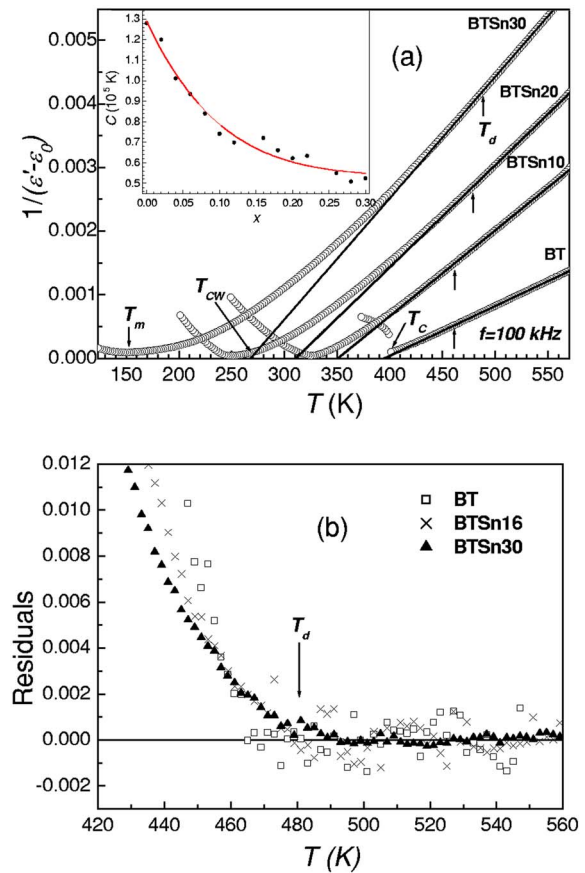


FIG. 8. (Color online) (a) Reciprocal of dielectric constant $[1/(\varepsilon' - \varepsilon_0)]$ as a function of temperature at 100 kHz for the BT, BTSn10, BTSn20, and BTSn30 ceramics. Solid lines are the fittings to the CW law, Eq. (3). Upward arrows indicate the temperature T_d below which ε' starts to deviate from the CW law. Inset is the CW parameter C as a function of the Sn content. (b) Residuals of the fitting to the CW law for selected compositions.

law is satisfied in all samples. Both parameters, T_{CW} and C , decrease smoothly with increasing Sn content, as shown in Figs. 2 and 8(a) (inset), respectively. ε_0 is found to be zero in BT but ranges from 20 to 166 in the Sn-substituted samples. Figure 2 also shows the variation of T_d as a function of x . Even in pure BT, a slight but noticeable deviation from the CW law is observed within a temperature interval of about 60 K above T_C , in agreement with the previous studies of BT ceramics^{32,33} [in pure BaTiO_3 crystals a departure from the CW law was found only in the interval of a few degrees above T_m (Refs. 34 and 35)]. Interestingly, T_d increases slightly from BT to BTSn04, and then remains constant at about 485 K.

Note that the CW behavior in the BTSn ceramics was reported in several works with the contradictory values of the CW parameters.^{21,23,30} For example, for $x=0.12$ the values of C were reported to be $(1.5, 1.7, \text{ and } 3.35) \times 10^5$ K in Refs. 23, 21, and 30, respectively. The reason for this discrepancy is that in all these studies the data were fitted to the CW law at too low temperatures (lower than T_d), which as we have shown is not accurately valid. Consequently the parameters obtained should depend on fitting temperature interval (which was actually different in different works cited above).

IV. DISCUSSION

Let us now discuss the possible mechanisms of dielectric response and doping-induced crossover from the DPT to relaxor behavior in the BTSn system. The fact that the CW law is valid in the paraelectric phase (i.e., at $T > T_d$) of all solid solutions and the parameters of the law change smoothly with x suggests that the origin of the paraelectric permittivity (or at least the origin of the dominating contribution to the permittivity) is the same as in the paraelectric phase of the pure BT. The lattice (soft phonon) contribution to the dielectric constant is responsible for the CW-type paraelectric permittivity in BT,^{36,37} and so is it in BTSn. Note that in this respect the behavior of BTSn can be considered similar to that of perovskite relaxors: lattice permittivity is also found to dominate in the paraelectric phase of PMN.^{38,39} The deviation from the CW law in relaxors is usually explained by the existence of small spontaneously polarized clusters (in PMN they have a size of a few nanometers) which appear below T_d . The same explanation is suitable for BTSn. Microscopically the formation of polar clusters can be understood in terms of the model of ferroelectric phase transitions in disordered crystals developed in Ref. 40. The existence of the polar clusters in BTSn is also confirmed by the transmission electron microscopy⁴¹ and by the observation of the ferroelectric-type hysteresis loops at temperatures much higher than T_m .^{23,42} One may further extend the analogy with classical relaxors by noticing that T_d is constant in a wide range of x (Fig. 2) even though T_m varies considerably. The similar behavior has been reported in PLZT solid solution system by Burns and Dacol⁴³ (the temperature of polar region formation T_d was determined in this work from the temperature dependence of the optic index of refraction) and in the solid solutions between PMN and PbTiO₃.⁴⁴ Therefore the state in the BTSn solid solution with $x > 0$ is analogous at $T < T_d$ to the ergodic relaxor state in classical relaxors. Nevertheless, we use the term “ergodic polar cluster state” to describe it (see Fig. 2), because on further cooling only compositions with large x become relaxors. The ergodicity becomes broken at some temperatures higher than T_m as confirmed by the appearance of the ferroelectric hysteresis loops^{23,42} and the piezoelectric effect in prepoled samples²¹ not only at $T < T_m$ but also in some temperature interval above T_m .

While the polarization mechanism contributing to the dielectric response at high temperatures seems to be the same for all the BTSn compositions studied, and thus the concentration dependences of the dielectric parameters of the paraelectric phase (T_{CW} , C , and T_d) do not show any anomalies, the low-temperature behavior is very different. It is obvious that the onset of strong dielectric dispersion leading to $T_m(f)$ dependence as well as the anomalies on the $T_m(x)$ and $W2/3M-L(x)$ curves indicate the same borderline of $x_c \approx 0.19$, above which the BTSn system starts to show relaxor behavior. The question thus arises how the single polarization mechanism contributing to the dielectric response in the paraelectric phase evolves upon cooling.

Different approaches were used in the literature to study the nature of the dielectric response in the vicinity of T_m in

BTSn. The $\varepsilon'(T)$ peaks in the compositions with moderate concentration of Sn are much higher than in pure BT (see Fig. 1). This was explained as the consequence of the change from the first-order phase transition in BT to the second-order transition in BTSn with $x \sim 0.1$.²³ In the case of second-order transition T_m is known to coincide with T_{CW} (such kind of coincidence was really found for BTSn10 in Ref. 23) and according to the CW law the dielectric constant should diverge at $T_m = T_{CW}$. The other evidence for the second-order phase transition presented in Ref. 23 was the absence of latent heat at T_m . However, our data do not confirm the fulfillment of the relation $T_m = T_{CW}$ for $x \sim 0.1$ or larger (see Fig. 2 and the discussion above). Besides, the absence of noticeable latent heat is the characteristic feature of all diffuse ferroelectric phase transitions regardless of the order.⁴⁵

The other approach, which we believe is more realistic, was suggested by Isupov,⁴⁶ who considered the dielectric constant of BTSn in the range of DPT as being composed of two contributions: the lattice susceptibility (the same as at $T > T_d$) and the susceptibility related to the relaxation of polar regions (which appear at $T < T_d$ as discussed above). This scheme can explain the dependence of ε_m on x . The lattice contribution at T_m is expected to decrease when x increases to approach to the relaxor compositions (in classical relaxors the lattice contribution to ε_m is known to be very small^{1,38}), but the contribution of polar clusters may increase (for the reasons to be discussed below). The total value of ε_m is defined by the balance of these two contributions and appears to have the maximum at $x \approx 0.1-0.2$.

To account for the ferroelectric-to-relaxor crossover we consider more closely the possible mechanisms of the dielectric relaxation of the polar clusters. Two such kinds of mechanisms are often discussed in the literature on relaxor ferroelectrics: reorientation of spontaneous dipole moments of clusters between the directions allowed by the crystal symmetry and the motion (“breathing”) of the cluster’s boundaries. The first mechanism can be realized only if the clusters are very small. Since the activation energy of the reorientation of the clusters is roughly proportional to their volume,² the large clusters cannot be reoriented by thermal motion and thus do not contribute to the (linear) dielectric response. According to the kinetic theory of the diffuse phase transitions in the compositionally disordered crystals,⁴⁷ the size of a newly appeared polar cluster is determined by the correlation length of phase transition order parameter (polarization in our case) and the correlation length is larger in ordered crystal than in disordered one.⁴⁷ Therefore the size of polar clusters in the BTSn solid solution with $x < x_c$ (small compositional disorder) is expected to be so large that the relaxation frequency resulting from the cluster reorientations is much smaller than the measurement frequency. As a result, only the relaxation of their boundaries contributes to the dielectric response. One may also expect that the characteristic time of this relaxation is significantly shorter than the highest frequency of 1 MHz used in our experiments [in relaxor PMN it is ~ 100 MHz or higher in the temperature range between T_m and T_d (Ref. 38)]. Therefore, we observe the static value of the cluster boundary susceptibility (χ_{b0}) with-

out any dispersion. It should be defined by the concentration of polar cluster boundaries in the bulk of the material which increases upon cooling because the size and number of clusters increase.⁴⁷ At low enough temperature the polar regions fill the major part of the crystal, some clusters merge into larger domains, some others form the domain walls with neighboring polar regions which leads to the decrease of the concentration of the interfaces between clusters and surrounding nonpolar matrix and thus to the maximum in the $\chi_{bo}(T)$ and $\varepsilon(T)$ dependences.

With increasing x the relaxation time of the polar cluster reorientation at $T \sim T_m$ decreases due to the decrease of their average size and becomes comparable with the inverse measurement frequency for $x > x_c$. The dielectric dispersion appears as a result. Therefore, the crossover between the DPT and the relaxor ferroelectric behavior is attributed to the appearance at $x > x_c$ of the additional dielectric contribution related to the flipping of the local polarization of polar clusters.

Note that using a picosecond soft x-ray laser speckle technique, comparatively large ($\sim 1 \mu\text{m}$) polarization clusters were recently observed even in pure BT up to temperatures as high as $T_m + 20 \text{ K}$.⁴⁸ These clusters are presumably responsible for the deviation from linearity of the temperature dependence of the index of refraction below $T_m + 180 \text{ K}$, which was discovered in BT crystals previously.⁴⁹ However, these clusters do not influence noticeably the dielectric permittivity. Indeed, the deviation from the CW law in the BT crystals was observed only in the very narrow vicinity of T_m (see discussion above) and therefore, the significant deviation found in the BT ceramics must have other origins. We speculate that dielectric response of the different types of polar clusters is different because the clusters observed in pure BT are fluctuating, i.e., they are not stable and their relaxation time (which is estimated in the range of nanoseconds⁴⁸) is their lifetime. In contrast, in BTSn with $x > 0$ (i.e., in compositionally disordered material), the stable polar clusters are theoretically possible⁴⁷ and practically realized. Their relaxation time is related to the thermally activated flipping of their dipole moments between different directions separated by the energy barriers and to the breathing of the boundaries of the polar regions. These processes give rise to the deviation from the CW law. As for the pure BT ceramics, the small deviation from the CW law in the interval of several dozens of degrees above T_m can be related to the dislocations, grain interfaces, and other structural defects, the concentration of which is expected to be larger in ceramics than in crystals. Such kind of defects can initiate the formation of polar regions at $T > T_m$, giving rise to the diffusion of the phase transition.⁴⁰ The relaxation of the boundaries of these regions can also account for the dielectric dispersion in the gigahertz frequency range in the same temperature interval where the deviation from the CW law is observed in the BT ceramics.³³

In conventional relaxors such as PMN, T_{VF} determined from the temperature dependences of the permittivity using Eq. (1) corresponds to the temperature of the freezing of the dynamics of polar nanoregions (PNRs) due to cooperative interactions between their moments.^{3,4} This is confirmed, in

particular, by the fact that the parameters T_{VF} , f_0 , and E_a coincide with the other parameters, T_f , f_{c0} , and U_a , respectively, determined from the frequency dependences of the permittivity using the other equation,

$$f_c = f_{c0} \exp[-U_a/k(T - T_f)], \quad (4)$$

where f_c is the characteristic frequency.^{4,50,51} The parameters $E_a = U_a$ and $f_0 = f_{c0}$ stand for the activation energy and the attempt frequency of the dipole reorientation, respectively. In the case of BTSn with $x \sim x_c$ the parameters E_a and f_0 are too small (see Fig. 5) to be interpreted in the same manner. On the other hand, the correspondence between the parameters of Eqs. (1) and (4) should not necessarily exist, and such a situation is even theoretically predicted in which Eq. (1) holds but Eq. (4) does not, e.g., the freezing of the dipole dynamics is absent.⁵² This situation is possible if the static permittivity has a temperature maximum and the relaxation spectrum broadens on cooling.⁵² These conditions are satisfied in BTSn. Therefore, we can conclude that the temperature T_{VF} has no direct relation to the glasslike freezing of the dielectric spectrum at least in the BTSn system with comparatively small x . To find out if the freezing really takes place in this system the frequency dependences of the permittivity should be properly analyzed. This work is currently in progress.

The prominent feature of the BTSn solid solution is the gradual increase of the diffuseness of the $\varepsilon(T)$ peak and thus the diffuseness of ferroelectric phase transition with increasing x starting from $x=0$. Even a small amount ($x=0.02$) of Sn leads to the noticeable smearing of the peak [see Fig. 7(a)]. This is in contrast to the classical lead-containing complex perovskite relaxors and their solid solutions in which the relatively diffuse maximum with its T_m obeying the VF law may be accompanied by a very sharp and frequency independent change of ε at temperatures several degrees below T_m .⁵³⁻⁵⁵ This discrepancy may also be explained by the large average size of polar clusters in the ergodic state (as suggested above). In the classical relaxors where the size of polar clusters is much smaller, the sharp change of ε related to the spontaneous relaxor to ferroelectric phase transition is explained by the sudden growth of some metastable polar clusters at a well-defined temperature (the same for every cluster).^{47,56} Many other (stable and dynamic) clusters merge into the growing ones to form macroscopic ferroelectric domains. In BTSn with small x the clusters are not dynamic (due to their large size) and the neighboring clusters having different directions of dipole moment cannot form the large (single) domains; in other words, the expansion of the growing cluster is hindered by the neighboring clusters. Other clusters begin to grow at different temperatures and consequently, the transition becomes diffuse.

V. CONCLUSIONS

Based on the dielectric spectroscopic studies, the T - x phase diagram of the $(1-x)\text{BaTiO}_3$ - $x\text{BaSnO}_3$ ($x=0$ -0.30) solid solution system has been established to reflect the ferroelectric and relaxor properties, as shown in Fig. 2. At high temperatures (in the paraelectric phase) the dielectric

constant follows the CW law (3) with the value of T_{CW} linearly decreasing with increasing x . The CW behavior in the paraelectric phase is presumably related to the softening of the lattice vibration mode, similar to the cases of the pure BT and the prototypical relaxor ferroelectric PMN. The deviation from the CW law is observed below the temperature T_d which is found to be the same (485 K) in all the compositions with $x \geq 0.04$ and slightly lower (460 K) in the pure BT. This deviation can be related to the formation at $T < T_d$ of dynamic and/or static polar regions embedded into non-polar surroundings. Therefore, the state of the material in this temperature range, which is called *ergodic polar cluster state*, is analogous to the relaxor ergodic state in classical relaxors. In agreement with this analogy, the characteristic Lorenz-type quadratic law (2) of relaxors is valid in the compositions with large x on the high-temperature slope of $\varepsilon'(T)$ peak between $T_Q \ll T_d$ and $T \approx T_m$. The interval of $T_Q - T_m$ decreases with decreasing x , and for x smaller than ~ 0.1 , becomes too small for unambiguous fitting with the quadratic law. While the dielectric behavior at $T > T_m$ is qualitatively the same for all compositions, in the close vicinity of T_m and below, very different behavior is observed in the samples with small and large x . At $x < x_c = 0.19$, T_m does not depend on frequency and the dielectric dispersion is comparatively small (except at very low frequencies where it is caused by the relaxation of mobile charges and thereby not ferroelectricity related). The solid solution with $x > x_c$ exhibits relaxor behavior with the frequency-dependent peak temperature T_m satisfying the VF law (1). Therefore, the critical composition x_c indicates the crossover from the diffuse ferroelectric phase transition to the relaxor ferroelectric behavior as the Sn content increases.

At this critical composition the anomaly (change of slope) in the linear $T_m(x)$ dependence is observed. At $x < x_c$, the parameter $W2/3M-L$ (proposed to describe the diffuseness in the ferroelectrics with DPT) increases linearly with increasing x , indicating that the sharp phase transition is observed only in pure BT and the $\varepsilon'(T)$ peak broadens gradually as the Sn content increases. This is in contrast to the behavior known in lead-containing complex perovskite relaxors where the diffuse (and sometimes dispersive) $\varepsilon'(T)$ maximum can be followed on cooling by the sharp drop of permittivity caused by the relaxor to ferroelectric phase transition. The dominating contributions to the $\varepsilon'(T)$ peak at $x < x_c$ are suggested to arise from the crystal lattice vibrations and from the relaxation of the boundaries of polar clusters. When x increases above x_c (in the relaxor part of the phase diagram) the additional dispersive contribution related to the reversal of polar cluster dipole moments appears. In classical relaxors the dipole dynamics related to the similar contribution freezes on cooling and the dipole-glass-like state appears at temperatures below T_{VF} . In BTSn, however, the VF shift of T_m has no direct relation to the glasslike freezing at least in the compositions with moderate x . The differences in the relaxor behavior between the BTSn solid solution and the lead-containing complex perovskite relaxors are explained in the framework of the kinetic theory of the diffuse phase transitions in the compositionally disordered crystals.

ACKNOWLEDGMENTS

This work was supported by the U.S. Office of Naval Research (Grant No. N00014-06-1-0166) and the Natural Sciences and Engineering Research Council of Canada (NSERC).

- ¹Z.-G. Ye, Key Eng. Mater. **155–156**, 81 (1998); A. A. Bokov and Z.-G. Ye, J. Mater. Sci. **41**, 31 (2006).
- ²L. E. Cross, Ferroelectrics **76**, 241 (1987).
- ³D. Viehland, S. G. Jang, L. E. Cross, and M. Wutting, J. Appl. Phys. **68**, 2916 (1990).
- ⁴A. E. Glazounov and A. K. Tagantsev, Appl. Phys. Lett. **73**, 856 (1998).
- ⁵J. Coutte, B. Dubus, J. C. Debus, C. Granger, and D. Jones, Ultrasonics **40**, 883 (2002).
- ⁶Z.-G. Ye and H. Schmid, Ferroelectrics **145**, 83 (1993).
- ⁷L. E. Cross, Ferroelectrics **151**, 305 (1994).
- ⁸G. Burns and F. H. Dacol, Solid State Commun. **48**, 853 (1983).
- ⁹X. Yao, Z. L. Chen, and L. E. Cross, J. Appl. Phys. **54**, 3399 (1984).
- ¹⁰D. Viehland, M. Wutting, and L. E. Cross, Ferroelectrics **120**, 71 (1991).
- ¹¹V. Westphal, W. Kleemann, and M. D. Glinchuk, Phys. Rev. Lett. **68**, 847 (1992).
- ¹²R. Pirc and R. Blinc, Phys. Rev. B **60**, 13470 (1999).
- ¹³A. A. Bokov and Z.-G. Ye, Phys. Rev. B **66**, 064103 (2002).
- ¹⁴K. Hirota, Z.-G. Ye, S. Wakimoto, P. M. Gehring, and G. Shirane, Phys. Rev. B **65**, 104015 (2002).
- ¹⁵S. Vakhrushev, A. Nabereznov, S. K. Sinha, Y. P. Feng, and T. Egami, J. Phys. Chem. Solids **57**, 1517 (1996).
- ¹⁶M. Yoshida, S. Mori, N. Yamamoto, Y. Uesu, and J. M. Kiat, Ferroelectrics **217**, 327 (1998).
- ¹⁷Z. Yu, C. Ang, R. Guo, and A. S. Bhalla, J. Appl. Phys. **95**, 2655 (2002).
- ¹⁸W. H. Payne and V. J. Tennery, J. Am. Ceram. Soc. **48**, 413 (1965).
- ¹⁹A. Chen, Y. Zhi, and J. Zhi, Phys. Rev. B **61**, 957 (2000).
- ²⁰J. Zhi, A. Chen, Y. Zhi, P. M. Vilarinho, and J. L. Baptista, J. Appl. Phys. **84**, 983 (1998).
- ²¹G. A. Smolenskii and V. A. Isupov, Zh. Tekh. Fiz. **24**, 1375 (1954).
- ²²G. A. Smolenskii, J. Phys. Soc. Jpn. **28**, 26 (1970).
- ²³N. Yasuda, H. Ohwa, and S. Asano, Jpn. J. Appl. Phys., Part 1 **35**, 5099 (1996).
- ²⁴R. Steinhausen, A. Kouvratov, H. Beige, H. T. Langhammer, and H.-P. Abicht, J. Eur. Ceram. Soc. **24**, 1677 (2004).
- ²⁵F. Jona and G. Shirane, *Ferroelectric Crystals* (Pergamon, New York, 1962).
- ²⁶X.-Y. Wei, Y.-J. Feng, and X. Yao, Appl. Phys. Lett. **83**, 2031 (2003).
- ²⁷A. Simon, J. Ravez, and M. Maglione, J. Phys.: Condens. Matter **16**, 963 (2004).
- ²⁸A. A. Bokov and Z.-G. Ye, Solid State Commun. **116**, 105 (2000).
- ²⁹A. A. Bokov, Y.-H. Bing, W. Chen, Z.-G. Ye, S. A. Bogatina, I. P. Raevskii, S. I. Raevskaya, and E. V. Sahkar, Phys. Rev. B **68**, 052102 (2003).
- ³⁰N. Baskaran and H. Chang, J. Mater. Sci.: Mater. Electron. **12**, 527 (2001).
- ³¹A. F. Devonshire, Philos. Mag. **40**, 1040 (1949).
- ³²S. Roberts, Phys. Rev. **75**, 989 (1949).
- ³³O. Kersten, A. Rost, and G. Schmidt, Ferroelectrics **81**, 31 (1988).
- ³⁴C. J. Jonson, Appl. Phys. Lett. **7**, 221 (1965).
- ³⁵J. A. Zvirgzds and J. V. Zvirgzde, Phys. Status Solidi B **101**, K21 (1980).
- ³⁶H. Vogt, J. A. Sanjurjo, and G. Rossbroich, Phys. Rev. B **26**, 5904 (1982).
- ³⁷E. Buixaderas, S. Kamba, and J. Petzelt, Ferroelectrics **308**, 131 (2004).
- ³⁸J. Petzelt, S. Kamba, V. Bovtun, and A. Pashkin, Ferroelectrics **298**, 219 (2004).
- ³⁹S. Kamba, M. Kempa, M. Berta, J. Petzelt, K. Brinkman, and N. Setter, J. Phys. IV **128**, 121 (2005).
- ⁴⁰A. A. Bokov, JETP **84**, 994 (1997).
- ⁴¹S. G. Lu, Z. K. Xu, and H. Chen, Appl. Phys. Lett. **85**, 5319 (2004).
- ⁴²C. Lei, A. A. Bokov, and Z.-G. Ye, Ferroelectrics **339**, 129 (2006).
- ⁴³G. Burns and F. H. Dacol, Phys. Rev. B **28**, 2527 (1983).
- ⁴⁴A. A. Bokov and Z.-G. Ye (unpublished).
- ⁴⁵F. Chu, I. M. Reaney, and N. Setter, J. Am. Ceram. Soc. **78**, 1947 (1995).
- ⁴⁶V. A. Isupov, Sov. Phys. Solid State **28**, 1253 (1986).
- ⁴⁷A. A. Bokov, Phys. Solid State **36**, 19 (1994).
- ⁴⁸R. Z. Tai, K. Namikawa, A. Sawada, M. Kishimoto, M. Tanaka, P. Lu, and K. Nagashima, Phys. Rev. Lett. **93**, 087601 (2004).
- ⁴⁹G. Burns and F. H. Dacol, Solid State Commun. **42**, 9 (1982).
- ⁵⁰A. Levstik, Z. Kutnjak, C. Filipič, and R. Pirc, Phys. Rev. B **57**, 11204

- (1998).
- ⁵¹A. A. Bokov and Z.-G. Ye, Phys. Rev. B **74**, 132102 (2006).
- ⁵²A. K. Tagantsev, Phys. Rev. Lett. **72**, 1100 (1994).
- ⁵³A. A. Bokov and S. M. Emelianov, Phys. Status Solidi B **164**, K109 (1991).
- ⁵⁴F. Chu, N. Setter, and A. K. Tagantsev, J. Appl. Phys. **74**, 5129 (1993).
- ⁵⁵A. A. Bokov, H. Luo, and Z.-G. Ye, Mater. Sci. Eng., B **120**, 206 (2005).
- ⁵⁶A. A. Bokov, Ferroelectrics **190**, 197 (1997).